Available online at www.sciencedirect.com

ScienceDirect

Geochimica et Cosmochimica Acta 276 (2020) 186–197

Geochimica et Cosmochimica Acta

www.elsevier.com/locate/gca

Cadmium and proton adsorption onto a halophilic archaeal species: The role of cell envelope sulfhydryl sites

Jinling Liu [a,b,*], Qiang Yu [b], Allison R. Showalter [c], Bruce A. Bunker [c], Juliet S. Swanson [d], Donald Reed [d], Xingmin Rong [e], Jeremy B. Fein [b,*]

[a] School of Earth Sciences, China University of Geosciences, Wuhan 430074, China
[b] Department of Civil & Environmental Engineering & Earth Sciences, University of Notre Dame, Notre Dame, IN 46556, United States
[c] Department of Physics, University of Notre Dame, Notre Dame, IN 46556, United States
[d] Repository Science and Operations, Los Alamos National Laboratory, Carlsbad, NM 88220, USA
[e] Key Laboratory of Arable Land Conservation (Middle and Lower Reaches of Yangtze River), Ministry of Agriculture, College of Resources and Environment, Huazhong Agricultural University, Wuhan 430070, China

Received 20 November 2019; accepted in revised form 27 February 2020; Available online 5 March 2020

Abstract

The adsorption of metal onto archaea could affect metal behavior and bioavailability in hypersaline environments where archaea represent the dominant life form. However, the mechanism and thermodynamics of metal adsorption onto halophilic archaea are not well understood. In this study, Cd adsorption experiments and potentiometric titrations were conducted to model metal adsorption by the halophilic archaeon *Halobacterium* sp.. Cd adsorption onto the archaeal cells exhibits slow adsorption kinetics, taking 8 h to reach steady-state. The extent of Cd adsorption depends strongly on pC_{H+} and Cd loading. Desorption of Cd is even slower than adsorption, but exposure of the Cd-adsorbed biomass to high concentrations of cysteine promotes desorption and demonstrates that the distribution of Cd is controlled by reversible adsorption reactions, likely involving sulfhydryl binding of Cd on the cell surface. We conducted potentiometric titration experiments with and without sulfhydryl site blocking to yield a total sulfhydryl site concentration of 91 ± 28 μmol/g within the archaeal cell envelope. Using a combination of the X-ray absorption fine structure analysis results from Showalter et al. (2016) and the Cd adsorption measurements and titration data from this study, we construct a surface complexation model of the Cd adsorption behavior. Because the Cd adsorption behavior is likely similar to that of a range of chalcophilic micronutrients, the importance of Cd-sulfhydryl binding suggests that the production of high affinity sulfhydryl binding sites by the archaea may represent an adaptive strategy for halophiles to obtain metal nutrients in environments in which aqueous metal-chloride complexation dominates the speciation for many metals.

Keywords: Archaea; Metal adsorption; Metal desorption; Sulfhydryl sites

1. INTRODUCTION

Microorganisms play critical roles in affecting the distribution, speciation and mobility of metals in near-surface geologic systems (Gadd, 2010). Adsorption of metal onto microbial surfaces contributes to biomineralization and bioaccumulation processes and in general can control metal bioavailability to microorganisms and affect the fate of

* Corresponding authors at: School of Earth Sciences, China University of Geosciences, Wuhan 430074, China. Fax: 027 67883002 (Jinling Liu). Fax: 574 631 9236 (J.B. Fein).
E-mail addresses: liujinling@cug.edu.cn (J. Liu), fein@nd.edu (J.B. Fein).

https://doi.org/10.1016/j.gca.2020.02.038
0016-7037/

metals in environment (Labrenz et al., 2000; Dunham-Cheatham et al., 2011).

Metal biosorption onto a wide range of bacterial species has been studied, yet these diverse species exhibit similar metal adsorption behaviors as a function of pH, ionic strength and metal loading (Yee and Fein, 2001; Borrok et al., 2004; Burnett et al., 2006; Ams et al., 2013). A limited range of functional groups, including phosphoryl, amino, hydroxyl, carboxyl, and sulfhydryl sites have been found to be responsible for metal adsorption (Yee and Fein, 2001; Fang et al., 2010; Mishra et al., 2010; Yu and Fein, 2015; Sun et al., 2016). Although not all bacterial sorption studies examine metal desorption behavior, some studies have documented full and rapid reversibility of bacterial metal adsorption reactions under high metal loading conditions where carboxyl and phosphoryl binding control metal adsorption on cell surfaces (Fowle and Fein, 2000; Ams et al., 2013; Yu and Fein, 2015). However, under low metal loading conditions where high affinity sulfhydryl binding controls adsorption (Mishra et al., 2010; Yu and Fein, 2015), only a portion of the adsorbed metal onto bacteria desorbs (Ledin et al., 1997; Yu and Fein, 2015).

Archaeal cells are distinct from bacteria in a number of ways. Archaeal cells lack a universal cell wall polymer and the lipids within archaeal cell membranes differ significantly in composition from bacterial lipid membranes (Ellen et al., 2010). Archaeal cell walls lack peptidoglycan, which is the rigid cell wall component in bacterial cell walls. In its place, some archaea have a crystalline protein layer and/or surface layer (S-layer) proteins (Albers and Meyer, 2011). Archaea are the predominant microorganisms in a range of extreme environments such as hypersaline, high temperature, or high radiation systems where most bacterial species cannot survive (Rothschild and Mancinelli, 2001; Lipp et al., 2008). Archaea that live in hypersaline environments may exhibit dramatically different metal adsorption strategies than non-halophilic bacteria. Archaeal cells need a cell envelope binding environment that enables cell envelope adsorption to compete for available metal cation nutrients with the aqueous metal-chloride complexation that occurs in these high chloride waters. Because of the difference in cell wall composition and the need for high affinity binding sites, the mechanisms responsible for metal adsorption onto halophilic archaea might differ from those that have been determined for bacteria.

Previous studies of metal adsorption onto archaea suggest that archaeal metal adsorption mechanisms are distinct from those exhibited by bacteria. Metal cation adsorption onto a range of halophilic archaea has been studied, with carboxyl, phosphoryl, amino, and sulfhydryl sites invoked to account for the observed adsorption behavior (Francis et al., 2004; Naik and Furtado, 2014; Bader et al., 2017; Bader et al., 2018). Although not observed for mesophilic bacterial species, U(VI) sorption onto some halophilic archaea occurs in a multistage process, likely an adsorption step followed by internalization or mineralization (Bader et al., 2017, 2018). Desorption experiments have been used to demonstrate that passive metal uptake by mesophilic bacteria is a reversible process that occurs on or near the cell surface (e.g., Fowle and Fein, 2000 Gorman-Lewis et al. 2019). Observed rapid and complete reversibility of Cu(II) adsorption onto an ammonia-oxidizing archaeal species, but there have been no desorption studies involving halophilic archaeal cells so the sorption mechanisms for halophilic archaea remain unknown.

In this study, we use Cd(II) and proton adsorption to probe metal binding mechanisms onto an aerobic halophilic archaeal species (*Halobacterium* sp. putatively *noricense*) that was isolated from salt deposits within the Waste Isolation Pilot Plant (WIPP) site. Considering that many halophilic archaeal species possess a high tolerance to Cd (up to 0.5 mM) (Voica et al., 2016), we use Cd as a surrogate divalent cation because of its relatively simple aqueous chemistry, with it present predominantly as Cd^{+2} across the pH range of interest. The interactions that we observe involving Cd^{+2} should be similar to those of other divalent cations, whether they are micronutrients or other toxic elements. We characterize the cells using transmission electron microscopy (TEM) and potentiometric titrations with and without sulfhydryl site blocking, and we conduct bulk Cd adsorption and desorption experiments as a function of time, pH, and Cd loading. We use the results from this study, in conjunction with those from our previous X-ray absorption fine structure (XAFS) spectroscopy experiments (Showalter et al., 2016), to determine the mechanisms and thermodynamics of Cd adsorption onto this archaeon. The objective of the research is to expand our understanding of how metals bind to halophilic archaeal species, and to improve our understanding of metal bioavailability to archaea in hypersaline systems.

2. MATERIALS AND METHODS

2.1. pH and pC_{H+}

The hydrogen ion activity is a critical factor influencing the interaction of metal and microbes. The traditional pH measurement by a standard combination pH electrode is widely applied in low ionic strength solutions. Because of interferences at the liquid junction of standard pH electrodes in high ionic strength solutions, however, the apparent pH reading does not reflect the real negative logarithm of the hydrogen ion concentration (pC_{H+}) in the experimental solutions. In this study, we correct the pH readings that we obtained from standard pH electrodes to pC_{H+} values using a relationship that depends directly on the ionic strength of the solution, following the approach developed by Rai et al. 1995 and Borkowski et al. 2009 and which is represented by the following equation:

$$pC_{H+} = pH_{measured} + (0.1868 \times I) - 0.073 \quad (1)$$

where *I* represents the ionic strength of the solution. In this study, the pH was measured using a standard pH electrode, and the corrected pC_{H+} values are reported throughout.

2.2. Archaeal growth and cell preparation

The studied archaeon *Halobacterium* sp. putatively *noricense* is an aerobic species, and was isolated from the WIPP site in a salt mine near Carlsbad, New Mexico, USA

(Swanson et al., 2012). A 3.4 M NaCl growth medium (Table S1) was used to culture the *Halobacterium* sp. cells during each growth step. After the medium was prepared and autoclaved, archaeal cells were first cultured aerobically in 3 mL of the sterilized medium at 32 °C for 7 days. This initial culture was then transferred to 2 L of growth medium of the same composition, and again cultured aerobically at 32 °C with agitation for 7 additional days to achieve early stationary phase (Fig. S1). After incubation, the archaeal cells were harvested by centrifugation at 8,100 g for 5 min, and rinsed three times with 3 M NaCl, with each rinse followed by centrifugation at 8,100 g for 5 min. Finally, the biomass pellets were transferred into pre-weighed test tubes and centrifuged for two 30-min intervals at 8,100 g, and the supernatant solution was decanted to yield a measurement of the wet archaeal biomass weight alone without solution present. We report all masses in terms of this wet biomass weight, but the wet weight to dry weight (defined as the biomass weight after 24 h in a 60 °C oven) conversion for this species was determined to be 2.4 ± 0.1. Conversions between our reported biomass concentrations and corresponding cell numbers as determined by manual direct counting of diluted bacterial suspensions are listed in Table S2.

2.3. Transmission electron microscopy

We used an epoxy and microtome approach in conjunction with TEM to image cross-sections of individual archaeal cells. After the above growth and washing procedure, the biomass pellet was suspended in a 2% gluteraldehyde fixative solution. The suspension was rotated end-over-end for 1 hour, then centrifuged and decanted. The pellet was rinsed three times with 3 M NaCl. The suspension was suspended in a 0.2% OsO_4 fixative solution and rotated end-over-end for 1 hour, then centrifuged at 8,100 g and decanted. The pellet was rinsed three times with 3 M NaCl, and then exposed to a series of ethanol solutions, starting at 50% ethanol and ending with 100% ethanol, to remove all water from the pellet. The dehydrated pellet was suspended in a series of Spurs resin solutions, starting with a 1:1 mixture of resin and 100% ethanol and ending with 100% resin, enabling infiltration of the cells with the resin. The infiltrated pellet was placed in the tip of a 1 mL BEEM capsule, and the capsules were filled with 100% resin and placed in a 70 °C oven for 24 h. The sample blocks were removed from the capsules, sectioned to 110 nm thickness, and mounted onto 200 mesh copper grids. TEM images were collected using a Hitachi H-600 TEM operated at 75 kV acceleration voltage.

2.4. Cadmium adsorption and desorption experiments

Sets of batch Cd adsorption experiments were conducted as a function of reaction time, metal loading (metal: biomass ratio), starting Cd concentration and pC_{H+}. Prior to the adsorption experiments, a commercial 1000 mg/L Cd $(NO_3)_2$ standard solution was diluted to the desired Cd concentration using 3 M NaCl. The pre-weighed archaeal cell pellet was then suspended in the diluted Cd solution using a vortex mixer to reach the desired concentration of archaeal cells. The well mixed Cd-biomass suspension was then divided into 10 mL aliquots in polypropylene test tubes, and the pC_{H+} of the suspensions was adjusted using small amounts of 1.0 M NaOH or HNO_3 in order to attain the desired pC_{H+} for each experimental suspension. One set of experiments was conducted at a fixed pC_{H+} of 7.2 and with Cd and cell concentrations of 66.7 μM and 100 g/L, respectively, with samples extracted periodically over 27 h. Based on these results, all subsequent experiments were allowed to react for 8 h for steady-state to be attained. The range of experimental pC_{H+} values was approximately 6.0–9.8, for experiments with 26.7 μM Cd, and cell concentrations of 10 g/L and 40 g/L. The experiments conducted as a function of Cd loading involved 3 M NaCl solutions with 66.7 μM Cd (pC_{H+} adjusted to 7.2), and cell concentrations ranging from 10 g/L to 135 g/L. In each experiment, the reaction vessels were placed on a rotating wheel with 10 rpm, and pC_{H+} was monitored during the experiment, and adjusted as needed. After the 8 h equilibration time, the final pC_{H+} was recorded. The samples were centrifuged at 8,100 g for 5 min and the supernatant was filtered through 0.45 μm nylon filter membranes to separate the cells from the solution. The filtered supernatant was diluted to approximately 0.3 M NaCl using ultrapure (18 MΩ) water and acidified with 2% nitric acid.

In addition to the adsorption experiments described above, three sets of desorption experiments were conducted: (1) desorption promoted by decreasing pC_{H+} after an initial adsorption step; (2) desorption promoted by the addition of a relatively low concentration of A-cysteine after an initial adsorption step; and (3) desorption promoted by the addition of a much higher concentration of A-cysteine after an initial adsorption step. The three desorption experiments were designed to promote desorption, with an increasing driving force for desorption from the pC_{H+} adjustment experiments providing the smallest driving force to the high concentration A-cysteine experiments with the highest driving force, in order to probe the reversibility and strength of the bonds holding Cd to the biomass. In the acidification desorption experiments, Cd was first adsorbed in a system containing 26.7 μM Cd in 3 M NaCl and 10 g/L of cells, allowing 8 h for adsorption steady-state to be reached, with pC_{H+} maintained at 9.6 for the duration of the adsorption step. After the 8 h adsorption step, the solution was sampled to determine the extent of Cd adsorption, and then the remaining cell suspension was divided into separate reaction vessels and the pC_{H+} of each system was adjusted downward to pC_{H+} values of 7–8.5 using small aliquots of 1 M HNO_3 to promote desorption. After 13 h of additional reaction time with rotation of the vessels, the final pC_{H+} of each system was measured, and the systems were sampled as described above to determine the concentration of Cd in each solution.

In the two cysteine-promoted desorption experiments, the initial adsorption step involved creating a pC_{H+} 6.7 cell suspension with a concentration of 40 g cells/L and containing 26.7 μM Cd and 3 M NaCl, and allowing equilibration to proceed for 8 h. After 8 h, the solution was sampled

as described above, and the biomass was re-suspended in either a 200 μM (for the low concentration experiments) or a 25 mM (for the high concentration experiments) A-cysteine solution with 3 M NaCl and pC_{H+} adjusted to 6.7. Each system was allowed to react for approximately 12 h, and then was sampled as described above, and duplicates of each were conducted.

Analyses of all the filtered acidified aqueous samples from the adsorption and desorption experiments were performed using inductively coupled plasma-optical emission spectroscopy (ICP-OES) (Perkin Elmer Optima 8000) with matrix-matched Cd standards in order to determine the total aqueous Cd concentrations in each sample. Repeat analyses of the Cd standards yielded an analytical uncertainty of ±2%. In addition, two different sets of control experiments were conducted: (1) to test for potential release of Cd from *Halobacterium* sp. in the absence of added Cd, and (2) to test for the loss of Cd from solution in the absence of *Halobacterium* sp. cells over the pC_{H+} range of 6.5–9.8.

2.5. Potentiometric titration experiments

In order to determine the total concentration of binding sites and the concentration of sulfhydryl binding sites within the cell envelope of *Halobacterium* sp., we conducted potentiometric titrations (T70 autotitrator, Mettler Toledo Inc.) on two different types of biomass samples: biomass treated with monobromo (trimethylammonio) bimane bromide (qBBr), which blocks the sulfhydryl sites within the cell envelope, and untreated biomass (Joe-Wong et al., 2012; Yu et al., 2014). The potentiometric titrations provide precise measurements of total site concentrations (Yu and Fein, 2016, 2017), so the difference in the total site concentration from the titrations with treated and untreated biomass yields the concentration of sulfhydryl sites on the cells. qBBr is not proton-active, it effectively blocks cell envelope sulfhydryl sites, and it does not react with other sites (e.g. carboxyl or phosphoryl sites) within the cell envelope (Yu et al., 2014). The qBBr treatment procedure for the archaeal cells is described briefly as follows: the NaCl-washed archaeal pellets were suspended in a freshly prepared qBBr solution in 3 M NaCl with pC_{H+} buffered to 7.5 ± 0.1 using a 1.8 mM Na_2HPO_4/1.82 mM NaH_2PO_4 buffer, with a qBBr: biomass ratio of approximately 100 μmol qBBr/g wet biomass, and the mixture was allowed to react for 8 h at room temperature in the dark and with continuous shaking on a rotating plate at 60 rpm. As shown in this study, Cd adsorption steady-state for the archaeal cell requires at least 8 h of reaction time. In our preliminary experiments (data not shown), we compared qBBr reaction times of 2 h and 8 h, and found that 8 h was needed for complete qBBr adsorption onto the sulfhydryl sites of the archaeal cell envelope.

Prior to the titrations, a 3 M NaCl solution in which the titration was to be conducted was degassed by bubbling N_2 for at least 1 h to remove dissolved CO_2. Meanwhile, the pH electrode was calibrated using NIST standard buffer solutions with pH values of 1.68, 4.01, 7.00, and 10.01, and the reported pC_{H+} was calculated by Eq. (1) (Borkowski et al., 2009; Ams et al., 2013). Archaeal cells with or without qBBr treatment were vortexed into the degassed 3 M NaCl solution to achieve a homogeneous suspension with a cell concentration of approximately 10 g/L. Throughout each titration, the suspension was continuously stirred with a magnetic stir bar, and N_2 was allowed to flow into the headspace above the suspension to prevent the influx of CO_2 to the suspension. Titrant additions of approximately 0.5 to 1.0 μL were added after a system stability of 0.01 mV/s was attained, with a minimum and maximum equilibration time of 60 and 180 s, respectively. For each biomass sample, two titration steps were conducted: (1) an 'up titration' during which the archaeal suspension pC_{H+} was adjusted up to 10.0 by adding 1.000 +/− 0.005 M NaOH standard; and (2) a 'down titration' from pC_{H+} 10.0–6.0 using a 1.000 +/− 0.005 M HCl standard as titrant. The down titration data were used for calculating the total site and sulfhydryl site concentrations, and four replicate titrations were conducted each with treated and untreated biomass samples. In preliminary experiments, several reverse titrations from pC_{H+} 6.0 to 10.0 were conducted immediately following the down titrations in order to test the reversibility of the protonation reactions. The resulting up titration curves matched well with their corresponding down titrations, indicating that no significant damage occurs to the cells during titrations between pC_{H+} 6.0 to 10.0 (results not shown). In order to compare results from titrations with different amounts of biomass, the titration results are plotted in terms of the mass normalized net concentration of protons added to the system:

$$[H^+]_{netadded} = (C_a - C_b)/m \quad (2)$$

where C_a and C_b are the total concentrations of acid and base added to the system during the titration, respectively, and m is the mass of the archaea in the suspension.

We model the proton-active functional groups on archaeal cell envelopes as discrete monoprotic acids, whose deprotonation reactions can be expressed using the following reaction (Fein et al., 2005; Yu and Fein, 2017):

$$R - A_iH^0 \leftrightarrow R - A_i^- + H^+ \quad (3)$$

where R denotes the archaeal cell envelope macromolecule to which the i^{th} organic acid functional group type, A_i, is attached. The acidity constant ($K_{a,\,i}$) and the total concentration (C_i) of the i^{th} site can be expressed as:

$$K_{a,i} = \frac{[R - A_i^-]\alpha_{H^+}}{[R - A_iH^0]} \quad (4)$$

$$C_i = [R{-}A_i^-] + [R - A_iH^0] \quad (5)$$

where $[R\text{-}A_i^-]$ and $[R\text{-}A_iH^0]$ represent the concentrations of the deprotonated and protonated ith organic acid functional group on the bacterial cell envelope, respectively, and α_{H+} is the activity of H^+ in the bulk solution.

Based on proton mass balance, the concentration of protons added to the system at any point of the titration can be described as (Fein et al., 2005):

$$C_a - C_b = [H^+] + \sum[R - A_iH^0] - T_H^0 - [OH^-] \quad (6)$$

where T_H^0 represents the initial proton concentration at the commencement of the titration and is solved for as a model

output parameter, [X] represents the concentration of species X in the experimental system, including H^+, OH^- and all the protonated organic acid functional groups within the archaeal cell envelope ($\sum$[R-A_i H^0]). We use a non-electrostatic surface complexation model for this exercise (Fein et al., 2005), and the computational tool FITEQL 2.0 (Westall, 1982), to model the potentiometric titration data.

2.6. Cell exudate experiments

Exudate solutions were prepared by suspending archaeal cells in 3 M NaCl solutions at pC_{H+} of 7.5 or 9.5, at a concentration of 10 g/L, allowing the cells to soak for either 1.5 h or 8.0 h, and separating the cells by centrifugation. Samples of the aqueous phase were taken periodically and measured for total dissolved organic carbon using a Shimadzu TOC-V instrument. After the archaeal cells were removed from the electrolyte soaking solution via centrifugation, the remaining supernatant contained material from the cell surface and/or material from the cell cytoplasm which entered solution as a result of cell lysis or passive excretion. Although it is possible that some of the exuded organics were colloidal, we refer to them as dissolved and define that to include all material in the supernatant that is not removed by our centrifugation step.

3. RESULTS

3.1. Characteristics of *Halobacterium* sp. cells

Fig. 1 depicts a representative TEM image of the *Halobacterium* sp. cells, grown under our experimental conditions. The cells have radii of approximately 250–450 nm, with distinctly visible cell walls with a thickness of approximately 15 nm. Some cells in Fig. 1 exhibit holes in their cell walls likely due to cell lysis during TEM sample preparation, and all cells in Fig. 1 exhibit desiccated cytoplasm adhering to the interior of the cell walls, also likely a sample preparation artifact. Note that there is little or no extracellular material visible in the biomass under the experimental conditions. After 1.5 h and 8.0 h at pC_{H+} of 7.5, the cells exuded 22.9 ± 1.1 and 36.2 ± 2.9 ppm DOC, respectively. After 8.0 h at pC_{H+} of 9.5, the cells exuded 109.4 ± 2.0 ppm DOC. We did not determine the molecular weight of the DOC, which likely stems from some cell lysis during the experiments, and hence we cannot determine the molality of DOC-hosted proton-active binding sites. However, bacterial cells exude similar mass-normalized DOC concentrations, and for bacterial exudates, proton-active binding sites are present within DOC at a level of less than 10% of the concentration of proton active sites on the cells (Seders and Fein, 2011).

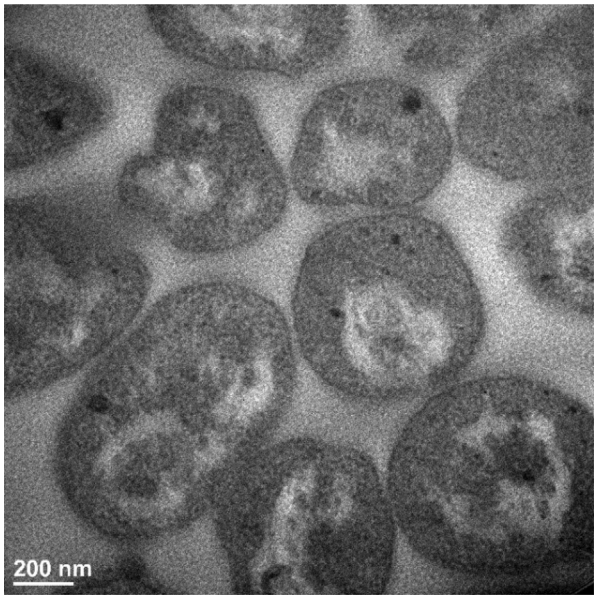

Fig. 1. Transmission electron microscopy (TEM) image of the halophilic archaeon *Halobacterium* sp. The dark grey material in the cell interior is cytoplasm, with nuclear material dispersed throughout the lighter portion of the cell interior.

3.2. Cd adsorption experiments

Our control experiments indicated that there is negligible release of Cd from the archaeal cells over the pC_{H+} range of the experiments, and that no appreciable loss of Cd from solution occurs in biomass-free systems or in cell-free exudate-bearing systems. The results from the kinetics experiments (Fig. 2a) indicate that the Cd adsorption reaction on the archaeal surface requires up to approximately 8 h to reach steady-state. The percentage of total Cd that adsorbs onto *Halobacterium* sp. under Cd loadings ranging from 0.49 to 6.67 μmol Cd/g archaea at pC_{H+} 7.2 decreases with increasing Cd loading (Fig. 2b). At 6.67 μmol Cd/g archaea, only a small percentage of the total Cd adsorbs onto *Halobacterium* sp., indicating that the number of Cd sorption sites on the archaeal cell wall are limited and that the available binding sites are nearly saturated. In addition, the adsorption capacity of *Halobacterium* sp. For Cd(II) is calculated to be 78.3 ± 12.6 μg/g wet biomass at pC_{H+} 7.2 (Fig. 2c) using $Q_e = \frac{V(C_0 - C_{eq})}{m}$, where V is the volume of the suspension, C_0 and C_{eq} are the initial and equilibrium solution Cd concentrations and m is the archaeal mass. In contrast, non-halophilic bacteria exhibit adsorption capacities for Cd(II) that are nearly three orders of magnitude higher (for example, 8 mg Cd /g wet *Bacillus subtilis* and 7 mg Cd /g wet *Shewanella oneidensis*, both at pH 5.9 or pC_{H+} 5.8) (Mishra et al., 2010).

Halobacterium sp. exhibits typical pC_{H+} dependent Cd adsorption behavior over the pC_{H+} range of 6 to ~10 (Fig. 2d), with adsorption generally increasing with increasing pC_{H+}, except for the lower Cd loading experiments which plateau at approximately 90% of the total Cd adsorbed onto the archaeal cells above pC_{H+} 7.5. Fig. 3 depicts the results from the desorption experiments conducted at a Cd loading of 2.67 μmol/g. Approximately 57% of the aqueous Cd was adsorbed during the initial adsorption step at pC_{H+} 9.6.

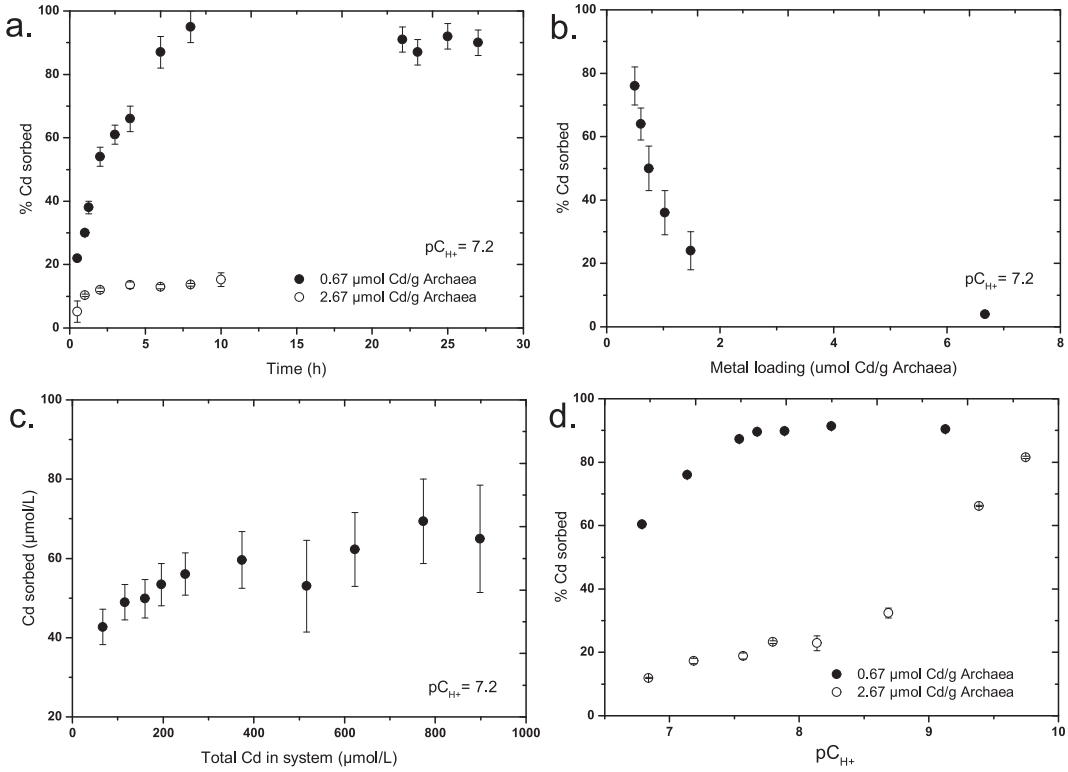

Fig. 2. Adsorption of Cd onto *Halobacterium* sp. in 3 M NaCl at pC_{H+} = 7.2 as a function of: (a) time, with [Archaea] = 100 g/L, [Cd] = 66.7 μM; and with [Archaea] = 10 g/L, [Cd] = 26.7 μM; (b) metal loading, with [Archaea] = 10–135 g/L, [Cd] = 66.7 μM, pC_{H+} = 6.7; (c) total Cd concentration, with [Archaea] = 100 g/L, [Cd] = 66.7–899 μM; and (d) pC_{H+}, with [Archaea] = 10 g/L and 40 g/L, [Cd] = 26.7 μM. Error bars represent 1σ uncertainties. Results from Panel (c) are from Showalter et al. (2016).

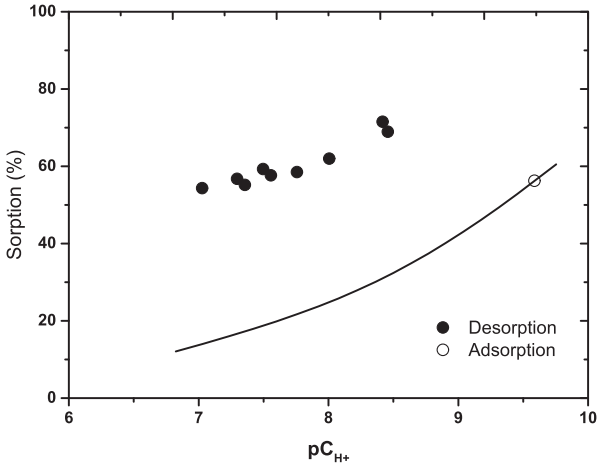

Fig. 3. Desorption of Cd onto *Halobacterium* sp. in 3 M NaCl as a function of pC_{H+}, with [Cd] = 26.7 μM, and [Archaea] = 10 g/L. The solid curve is a smoothed fit to the adsorption data shown in Fig. 2d. The open circle represents the measured extent of Cd adsorption prior to the desorption step.

3.3. Cd desorption experiments

In the experiments in which desorption was promoted by acidification, approximately 57% of the aqueous Cd was sorbed during the initial sorption step at pC_{H+} 9.6. Although the pC_{H+} of the systems was decreased to promote desorption, there was no reversal of the sorption reaction even when pC_{H+} was dropped to 7, a condition at which less than 20% of the Cd sorbed in our sorption experiments (Fig. 3). Similarly, in the low concentration A-cysteine-promoted desorption experiments, the initial sorption step led to 37% and 30% removal of Cd from solution in the two duplicate experiments, but the addition of 200 μM cysteine did not cause significant desorption of Cd over the 12 h of desorption reaction time. The initial adsorption step in the high concentration A-cysteine desorption experiment yielded adsorption of 73 ± 2% of the Cd in the system. In these experiments, the biomass was separated and re-suspended in a 25 mM A-cysteine solution, and after an 8 h exposure time, an average of 86 ± 1% of the biomass-associated Cd desorbed and was present in solution.

3.4. Determination of sulfhydryl site concentration on the archaeal cells

Showalter et al. (2016), studying Cd adsorption onto *Halobacterium* sp. under similar conditions to those in this study using X-ray adsorption near-edge spectroscopy (XANES) and extended X-ray absorption fine structure (EXAFS), found that sulfhydryl sites within the cell envelope dominate Cd adsorption onto *Halobacterium* sp. at pC_{H+} of 7.2. In order to construct quantitative models of

Cd adsorption onto the archaeal cells, we first measured the concentration and acidity constants for these sulfhydryl sites. Our potentiometric titration experiments, conducted with and without qBBr blocking of cell envelope sulfhydryl sites, yield these parameters. The titration experiments show that *Halobacterium* sp. cell suspensions possess substantial buffering capacity over the pC_{H+} range from 6.0 to 10.0 (Fig. 4), similar to the behavior reported for mesophilic and thermophilic bacteria and thermophilic archaea (Fein et al., 1997; Daughney et al., 2010).

In this study, we used FITEQL 2.0 to model the titration data and to optimize unknown parameters (e.g. T^0_H, $K_{a,i}$ and C_i) (Fein et al., 2005). We used a non-electrostatic surface complexation modeling approach due to a lack of constraints on the effects of ionic strength, testing models that involved one, two, three and four binding site types, each with distinct p*K*a values, to fit the potentiometric titration data. A two-site model provides the best fit to each of the titration datasets, for both the untreated and the qBBr-treated biomass samples (Fig. 4). The protonation behavior of *Halobacterium* sp. can be described with 2 proton-active sites with p*K*a values of 6.36 ± 0.03 and 9.71 ± 0.16 (Table 1). The Student's T test shows that the total site concentration of qBBr-treated biomass is significantly different ($P < 0.05$) from the untreated biomass. The difference in the total concentration of binding sites between the qBBr-treated and the untreated biomass represents the concentration of sulfhydryl binding sites (91 ± 28 μmol/g wet biomass) for *Halobacterium* sp. (Table 1). There is no significant difference (Student's T test, $P > 0.05$) in the Site 1 concentrations between the qBBr-treated and untreated samples, indicating either that Site 1 does not contain sulfhydryl sites or that the concentration of sulfhydryl sites with the same p*K*a value as Site 1 is below the detection limit of the potentiometric titration method (approximately10 μmol/g wet biomass). In contrast, the Site 2 concentration changes significantly between the untreated and the qBBr-treated biomass samples ($P < 0.01$), indicating a significant sulfhydryl contribution to the site with a p*K*a value of between 9.5 and 10.

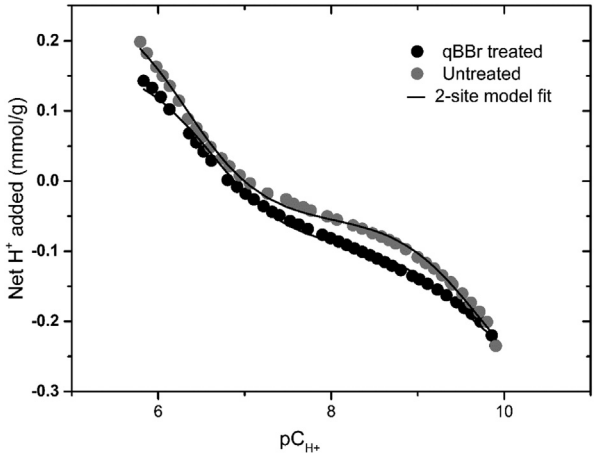

Fig. 4. Representative potentiometric titrations conducted with untreated biomass (grey circles) and with qBBr-treated biomass to block cell envelope sulfhydryl sites (black circles). The solid curves in each case depict the best-fitting model to the data.

Table 1
Summary of binding site concentrations within the cell envelope of *Halobacterium* sp. biomass samples from replicate potentiometric titrations. Reported uncertainties are 1σ values.

qBBr treatment	p$K_{a,1}$	p$K_{a,2}$	Site 1 μmol/g	Site2 μmol/g	Total μmol/g
Untreated	6.37	9.92	257	217	474
Untreated	6.33	9.75	262	213	475
Untreated	6.33	9.62	314	242	556
Untreated	6.40	9.55	342	243	585
Mean	**6.36**	**9.71**	**294**	**229**	**522**
σ	**0.03**	**0.16**	**41**	**16**	**57**
qBBr-treated	6.57	9.46	248	187	435
qBBr-treated	6.53	9.37	275	163	438
qBBr-treated	6.62	9.49	257	175	432
qBBr-treated	6.54	9.44	254	164	418
Mean	**6.56**	**9.44**	**259**	**172**	**431**
σ	**0.04**	**0.05**	**12**	**11**	**9**

4. DISCUSSION

4.1. Adsorption and desorption kinetics

The results from the kinetics experiments (Fig. 2a, b, c) indicate that the Cd adsorption reaction on the archaeal surface requires 8 h to reach steady-state, and depends strongly on pC_{H+} and metal loading. This reaction time is significantly longer than that required for other microbial-metal systems, including Cd adsorption by bacteria (Bartolucci et al., 2013; Boyanov et al., 2003; Burnett et al., 2006; Mishra et al., 2010) and Mn (Naik and Furtado, 2014) and U (Francis et al., 2004) adsorption by haloarchaea, each of which reach steady state adsorption in 2 h or less. The cause of the slower adsorption kinetics for Cd onto *Halobacterium* sp. relative to previously-studied microorganisms is unknown, but may be a result of a thicker cell wall on the *Halobacterium* sp. studied relative to previously-studied species, a higher cell density used in these experiments, active ion efflux out of the cell to maintain osmotic balance, and/or as a toxicity defense mechanism (Bartolucci et al., 2013). The pC_{H+} dependence likely is controlled by Cd binding onto deprotonated binding sites, which increase in availability with increasing pC_{H+}. The two desorption experiments which showed no reversal of the initial adsorption reaction (Fig. 3), suggest that adsorption reversibility is more difficult than has been observed for mesophilic bacterial cells, but that given a strong enough driving force for desorption, adsorption reversibility does occur and that modeling the adsorption process using an equilibrium thermodynamics approach is justified.

The first two desorption experiments suggest that the sorbed Cd is either internalized by the archaeal cells or is bound strongly onto some component of the cell envelope such that desorption occurs much more slowly than does the initial sorption step. However, the results from

the high concentration A-cysteine desorption experiments strongly suggest that the second explanation is correct, and that the Cd sorption reactions are reversible given enough of a driving force for desorption. The 25 mM A-cysteine desorption experimental results demonstrate that almost all of the biomass-sorbed Cd can be liberated, but the fact that A-cysteine, present in over a 1000-fold molar excess relative to Cd, does not liberate all of the biomass-associated Cd suggests that either a small fraction of the Cd (approximately 10% of the originally introduced Cd) is internalized, or that the biomass-associated Cd is attached to cell surface binding sites with especially high affinities for Cd. In fact, at least for bacterial binding of Cd, Cd-sulfhydryl surface complexes exhibit thermodynamic stabilities that are over three orders of magnitude greater than that of Cd surface complexes with non-sulfhydryl sites (Yu and Fein, 2015), and hence we conclude that our desorption experiments demonstrate extremely strong, but reversible binding behavior of the Cd onto the archaeal surface.

4.2. Sulfhydryl site concentration on the archaeal cells

The sulfhydryl site concentration that we measured for the *Halobacterium* sp. cell envelope is significantly higher than previously reported sulfhydryl site concentrations of Gram-positive and Gram- negative bacteria (typically 15–35 μmol/g wet biomass) (Joe-Wong et al., 2012; Kenney et al., 2012; Yu et al., 2014). The p*K*a value for the sulfhydryl site on the *Halobacterium* sp. cell envelope is between 9.5 and 10, which is similar to the range of typical p*K*a values for small thiol-bearing molecules (e.g., cysteine, glutathione, homocysteine) (approximately 8.0–10.0) (Walsh and Ahner, 2013), although the p*K*a values for sulfhydryl sites can shift to significantly lower values due to steric interactions between sulfhydryl sites and protonated amino or carbohydrate groups (Krader and Emerson, 2004; Antoine et al., 2006; Daughney et al., 2010). Additionally, the S-layer glycoproteins on *Haloarchaea* can contain S-bearing residues, possibly including sulfhydryl sites, and which may contain lower concentrations of phosphoryl groups and carboxyl groups than bacterial cell envelopes (Daughney et al., 2010). Our titration results indicate that sulfhydryl sites account for 18% of the total proton binding sites within the cell envelopes of *Halobacterium* sp., which is a higher proportion than is present in previously-studied bacterial cell envelopes, for which sulfhydryl sites typically represent only 5–10% of the total site concentration (Joe-Wong et al., 2012; Yu et al., 2014). The higher sulfhydryl site concentration of *Halobacterium* sp. seems to conflict with its lower adsorption capacity for Cd(II) relative to that exhibited by other microorganisms (e.g. *Bacillus subtilis*, *Shewanella oneidensis*). The lower extents of Cd adsorption by *Halobacterium* sp. likely reflect its lower concentrations of non-sulfhydryl sites (e.g., carboxyl, phosphoryl) relative to the concentration of these sites on bacteria and/or the effects of chloride competition for available Cd in the highly saline experimental systems.

4.3. Thermodynamic modeling of Cd adsorption onto the archaeal cells

The results from our desorption experiments suggest that Cd is strongly, yet reversibly bound onto the archaeal surface. The XAFS results from Showalter et al. (2016) suggest that Cd adsorption predominates under the experimental conditions with Cd precipitation occurring only under higher Cd loading conditions than were studied here (≥17 μmol Cd/g cells). Therefore, we use our range of experimental measurements to construct and calibrate a thermodynamic model of Cd adsorption onto the *Halobacterium* sp. archaeal cell envelope and to test if modeling Cd removal as adsorption reactions can explain the observed Cd removal behavior as a function of pC_{H+} and Cd: cell ratio. As noted above, the cells exude some DOC into solution, and it is possible that Cd binds onto proton-active sites on the DOC molecules thereby forming aqueous Cd-DOC complexes. Our modeling approach does not account for the formation of these aqueous complexes, and hence the stability constant values that we calculate for the Cd-archaea surface complexes represent minimum estimates.

The XAFS measurements under similar conditions to those studied here indicate that Cd binds onto both sulfhydryl and non-sulfhydryl sites within the archaeal cell envelope, that the Cd bound to the non-sulfhydryl sites has chloride in its binding environment, and that the average S coordination number of the bound Cd is 1.5–2.0 (Showalter et al., 2016). Our potentiometric titration data yield constraints on the p*K*a and site concentration of the sulfhydryl sites. The bulk adsorption measurements conducted as a function of Cd loading place additional constraints on the Cd: site ratio of the important surface complexes, and the adsorption measurements conducted as a function of pC_{H+} can be used to constrain the stability constants for the dominant Cd-archaeal surface complexes.

First, we use the Cd loading data to determine the reaction stoichiometry. Cd adsorption onto the cell wall of the archaea can be described using the following generic reaction:

$$Cd^{+2} + x[R - A_i^-] \leftrightarrow [R - A_i]_x - Cd^+ \quad (7)$$

where R-A_i– represents the deprotonated form of Site *i* (*i* = 1 or 2); $[R\text{-}A_i]_x\text{-}Cd^+$ represents the archaeal surface complex formed between the aqueous Cd cation (Cd^{2+}) and the deprotonated surface Site *i,* and x represents the stoichiometric coefficient for the deprotonated site involved. The goal of this initial modeling exercise is to determine the value of x that best fits the experimental Cd loading data and to test whether it is consistent with the EXAFS coordination number determination determined by Showalter et al. (2016). The reactions and *K* values involved in the modeling exercise are listed in Table S3. We use a non-electrostatic surface complexation model for this exercise (Fein et al., 2005), and the computational tool FITEQL 2.0 (Westall, 1982), to fit the Cd adsorption data as a function of Cd loading (Fig. 2b), using the average p*K*a values and site concentrations from the titration data (Table 1). In these calculations, FITEQL solves a set of

non-linear equations that represents the mass action and mass balance constraints on the system (Table S3). We test x values in Reaction (7) of 1 and 2, for Cd binding onto either the deprotonated form of Site 1 or Site 2. Based on the values of the FITEQL goodness-of-fit parameter, V (Y), a 1: 2Cd : Site stoichiometry yields a significantly better fit to the data than does a 1:1 stoichiometry (Fig. 5), with V (Y) values improving from 18 for the 1:1 stoichiometry to 1.6 for the 1:2 complex. This modeling result is consistent with the XAFS data which yield a coordination number of 1.6 ± 0.7 to1.9 ± 0.9 for adsorbed Cd on the archaeal surface (Showalter et al., 2016).

The following reactions account for the constraints on the adsorption mechanisms from the XAFS results and can be used to model the pC_{H+} dependence of Cd adsorption onto *Halobacterium* sp.:

$$CdCl^{+1.} + Site_1{}^{-1.} \leftrightarrow Site_1 - CdCl^0 \quad (8)$$

$$Cd^{+2.} + 2[R - S^{-1}] \leftrightarrow [R - S]_2Cd^0 \quad (9)$$

The equilibrium constants for these reactions can be expressed as:

$$K_{Cd-Site1} = \frac{[Site_1 - CdCl^0]}{[Site_1^{-1}]\alpha_{CdCl^{+1}}} \quad (10)$$

$$K_{Cd-Site2} = \frac{[(R - S)_2Cd^0]}{[R - S^{-1}]^2\alpha_{Cd^{+2}}} \quad (11)$$

where brackets represent concentrations of archaeal surface species, and α represents the activity of the subscripted aqueous species. We use the bulk Cd adsorption measurements conducted as a function of pC_{H+}, in conjunction with FITEQL 2.0 (Westall, 1982), to solve the set of mass action and mass balance constraints on the system and to yield values for the equilibrium constants for Reactions (8) and (9). Our potentiometric titration experiments indicate that a majority of the sulfhydryl sites within the archaeal cell envelope exhibit p*K*a values similar to those of what we term Site 2, with a p*K*a of 9.7. Therefore, in this modeling approach, we use 9.7 as the p*K*a value for the sulfhydryl sites, and we assign the sulfhydryl sites concentration equals to the difference in Site 2 concentrations for the qBBr-treated and untreated biomass samples (for a sulfhydryl site concentration of 57 μmol/g). Pitzer equations (Pitzer, 1973) were used to calculate activity coefficients for these high ionic strength (3 M NaCl) systems.

Reactions (8) and (9) account well for both the pC_{H+} and Cd loading dependencies to the bulk adsorption data (Fig. 6a and 6b). Under the lower Cd loading condition, the model predicts approximately equal concentrations for the two Cd-archaeal surface complexes at pC_{H+} 7.2, which are the conditions of the XAFS results from Showalter et al. (2016) which also yielded an approximately equal importance for the sulfhydryl-bound and non-sulfhydryl bound Cd fractions. Despite this good agreement for the low Cd loading condition, under the higher Cd loading, the thermodynamic model under-predicts the importance of the Cd-sulfhydryl complex relative to the XAFS data. Furthermore, the model yields log *K* values for Reactions (8) and (9) that change as a function of Cd loading (from 3.4 to 4.2 for $K_{(8)}$ between 2.67 and 0.67 μmol/g; and from 8.9 to 12.8 for $K_{(9)}$ for the two Cd loadings). The change in *K* values suggests that the adsorption reactions change significantly as a function of metal loading, and perhaps the 1:2 stoichiometry that we use in Reaction (9) changes to 1:1 under the higher metal:ligand loading condition. In addition, our assumption that all Cd-sulfhydryl binding occurs on a site with a p*K*a value of 9.7 may not be valid. Although the concentration of sulfhydryl sites with a lower p*K*a value was below the detection limit of our potentiometric titration approach, some sulfhy-

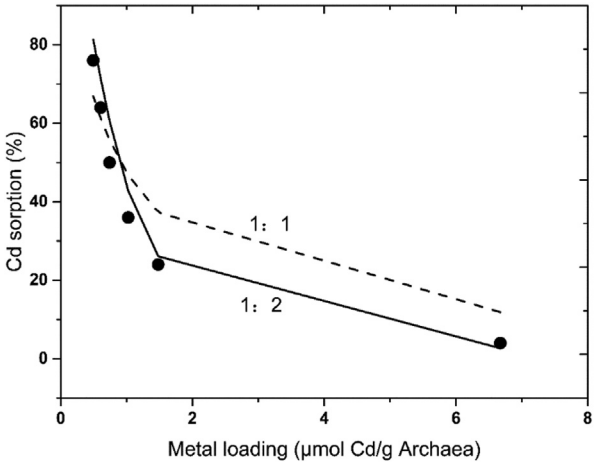

Fig. 5. Surface complexation modeling results: one-site model of Cd adsorption onto *Halobacterium* sp. cells as function of metal loading at pC_{H+} 7.2 for 1:1 and 1:2 Cd:site stoichiometries.

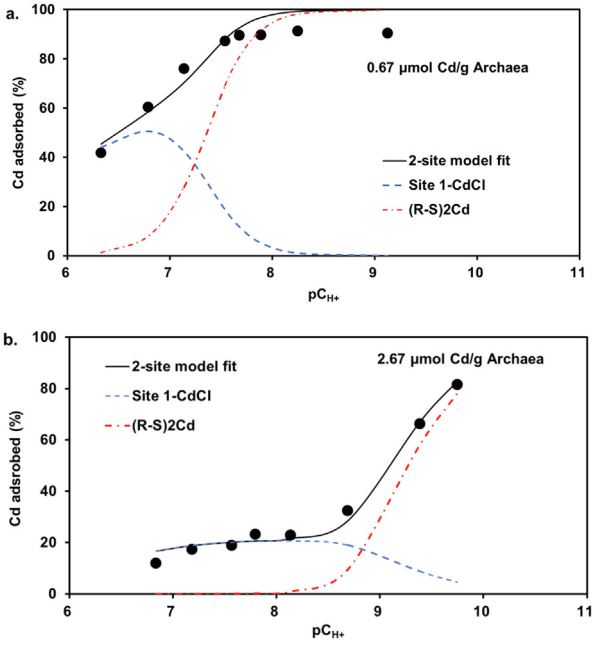

Fig. 6. Surface complexation modeling results: (a) best-fitting model of Cd adsorption onto *Halobacterium* sp. cells for experiments with a Cd loading of 0.67 μmol Cd/g wet biomass; and (b) best-fitting model for experiments with 2.67 μmol Cd/g wet biomass.

dryl sites may be present as part of Site 1, which would decrease the calculated importance of the Cd-chloride surface complex at pC_{H+} 7.2 relative to the Cd-sulfhydryl complex. Finally, the shift may reflect real differences in Cd binding with different types of sulfhydryl sites on the cell.

4.4. Function of sulfhydryl sites on *Halobacterium* sp.

The results from this study demonstrate the importance of sulfhydryl sites in the binding of Cd, and likely other chalcophile metals, onto the halophilic archaeon *Halobacterium* sp. Previous XAFS measurements on a system under similar conditions to those studied here (Showalter et al., 2016) indicate that Cd binding is dominantly due to complexation with sulfhydryl sites within the cell envelope over a range of Cd loading conditions. Our potentiometric titration experiments with and without qBBr blocking of cell envelope sulfhydryl sites yield a sulfhydryl site concentration that is significantly higher than those measured for non-halophilic bacterial species (Joe-Wong et al., 2012; Kenney et al., 2012; Yu et al., 2014). We speculate that sulfhydryl sites within the cell envelope are necessary for the archaea to be able to compete with aqueous chloride to bind available metal micronutrients that are chalcophile elements (such as Zn, Cu, Se, etc.). Under the aerobic growth conditions of our experiments, the reduced S that is present within sulfhydryl sites is not the thermodynamically stable form of S, and the cell therefore must expend metabolic energy to create sulfhydryl sites. Because sulfhydryl sites bond strongly with a number of essential nutrients which are chalcophilic such as Zn, Se, Co, Ni, etc., it is possible that the cell invests energy into creating sulfhydryl sites to attract the nutrients to the cell to become bioavailable. Halophilic archaea, living in solutions with such high concentrations of chloride, face an especially difficult task of attracting these metals because many of them form aqueous complexes with chloride which likely do not adsorb as readily as do the metal cationic species. Thus, the production of an abundance of sulfhydryl sites within the archaeal cell envelope could be the result of an evolutionary mechanism developed by the halophilic archaeon to obtain essential metal nutrients from environments in which aqueous metal-chloride complexation dominates the speciation for many metals.

5. CONCLUSIONS

The halophilic archaeon *Halobacterium* sp. exhibits a dramatically different metal adsorption strategy than non-halophilic bacteria. In a high chloride environment, Cd adsorption onto the archaeal cells is slower and less extensive than other previously-studied metal-microbe systems. The extent of Cd adsorption increases with decreasing metal loading and increasing pC_{H+}, and Cd desorption only occurs when a large driving force for desorption is created. Cd is present on the archaeal cells as two distinct surface complexes: an inner-sphere Cd-sulfhydryl complex and a non-sulfhydryl Cd-chloride complex. The total sulfhydryl site concentration on the archaeal cell is 92 ± 28 μmol/g which accounts for 18% of the total proton binding sites. We use our potentiometric titration data, the results of the Cd adsorption batch experiments, and the results from a previous XAFS study by Showalter et al. (2016) to develop a surface complexation model of the Cd adsorption behavior and to determine log K values for the important Cd-archaeal surface complexes for the two metal loading conditions studied. The importance of sulfhydryl sites in binding divalent cationic Cd suggests that these sites may also play an important role in the bioavailability of other chalcophile elements (e.g. Zn, Cu) as well. Thus, the production of high affinity sulfhydryl sites within the archaeal cell envelope could be an adaptive strategy for halophiles to obtain essential metal nutrients from environments in which aqueous metal-chloride complexation dominates the speciation for many metals.

Declaration of Competing Interest

The authors declare that they have no known competing financial interests or personal relationships that could have appeared to influence the work reported in this paper.

ACKNOWLEDGMENTS

Funding for this project was provided in part by U.S. National Science Foundation grants EAR-1424950 and EAR-1904192, the Natural Science Foundation of China (No. 41773112) and by the Fundamental Research Funds for the Central Universities, China University of Geosciences (Wuhan) (No. CUGCJ1703). The first author also gratefully acknowledges financial support from the China Scholarship Council. The ICP-OES analyses were conducted at the Center for Environmental Science and Technology (CEST) at University of Notre Dame, and partial support for A. Showalter was through a CEST pre-doctoral fellowship. The journal reviews and the suggestions by Associate Editor Oleg Pokrovsky were constructive and greatly improved the quality of the work.

APPENDIX A. SUPPLEMENTARY MATERIAL

Supplementary data to this article can be found online at https://doi.org/10.1016/j.gca.2020.02.038.

REFERENCES

Albers S. V. and Meyer B. H. (2011) The archaeal cell envelope. *Nat. Rev. Microbiol.* **9**, 414–426.

Ams D. A., Swanson J. S., Szymanowski J. E. S., Fein J. B., Richmann M. and Reed D. T. (2013) The effect of high ionic strength on neptunium (V) adsorption to a halophilic bacterium. *Geochim. Cosmochim. Acta* **110**, 45–57.

Antoine M., Gand A., Boschi-Muller S. and Branlant G. (2006) Characterization of the amino acids from *Neisseria meningitidis* MsrA involved in the chemical catalysis of the methionine sulfoxide reduction step. *J. Biol. Chem.* **281**, 39062–39070.

Bader M., Muller K., Foerstendorf H., Drobot B., Schmidt M., Musat N., Swanson J. S., Reed D. T., Stumpf T. and Cherkouk A. (2017) Multistage bioassociation of uranium onto an extremely halophilic archaeon revealed by a unique combination of spectroscopic and microscopic techniques. *J. Hazard. Mater.* **327**, 225–232.

Bader M., Muller K., Foerstendorf H., Schmidt M., Simmons K., Swanson J. S., Reed D. T., Stumpf T. and Cherkouk A. (2018)

Comparative analysis of uranium bioassociation with halophilic bacteria and archaea. *PLoS ONE* **13**, e0190953.

Bartolucci S., Contursi P., Fiorentino G., Limauro D. and Pedone E. (2013) Responding to toxic compounds: a genomic and functional overview of Archaea. *Front. Biosci.-Landmark* **18**, 165–189.

Borkowski M., Lucchini J. -F., Richmann M. K. and Reed D. T. (2009) Actinide (III) Solubility in WIPP Brine: Data Summary and Recommendations, Los Alamos National Laboratory, an affirmative action/ equal opportunity employer, is operated by Los Alamos National Security, LLC, for the National Nuclear Security Administration of the U.S. Department of Energy under contract DE-AC52-06NA25396.

Borrok D., Fein J. B. and Kulpa C. F. (2004) Proton and Cd adsorption onto natural bacterial consortia: Testing universal adsorption behavior. *Geochim. Cosmochim. Acta* **68**, 3231–3238.

Boyanov M. I., Kelly S. D., Kemner K. M., Bunker B. A., Fein J. B. and Fowle D. A. (2003) Adsorption of cadmium to *Bacillus subtilis* bacterial cell walls: a pH-dependent X-ray absorption fine structure spectroscopy study. *Geochim. Cosmochim. Acta* **67**, 3299–3311.

Burnett P.-G. G., Daughney C. J. and Peak D. (2006) Cd adsorption onto *Anoxybacillus flavithermus*: Surface complexation modeling and spectroscopic investigations. *Geochim. Cosmochim. Acta* **70**, 5253–5269.

Daughney C. J., Hetzer A., Heinrich H. T. M., Burnett P. G. G., Weerts M., Morgan H., Bremer P. J. and McQuillan A. J. (2010) Proton and cadmium adsorption by the archaeon *Thermococcus zilligii*: Generalising the contrast between thermophiles and mesophiles as sorbents. *Chem. Geol.* **273**, 82–90.

Dunham-Cheatham S., Rui X., Bunker B., Menguy N., Hellmann R. and Fein J. (2011) The effects of non-metabolizing bacterial cells on the precipitation of U, Pb and Ca phosphates. *Geochim. Cosmochim. Acta* **75**, 2828–2847.

Ellen A. F., Zolghadr B., Driessen A. M. J. and Albers S. V. (2010) Shaping the archaeal cell envelope. *Archaea-an Int. Microbiological J.*. https://doi.org/10.1155/2010/608243.

Fang L. C., Cai P., Li P. X., Wu H. Y., Liang W., Rong X. M., Chen W. L. and Huang Q. Y. (2010) Microcalorimetric and potentiometric titration studies on the adsorption of copper by *P. putida* and *B. thuringiensis* and their composites with minerals. *J. Hazard. Mater.* **181**, 1031–1038.

Fein J. B., Boily J.-F., Yee N., Gorman-Lewis D. and Turner B. F. (2005) Potentiometric titrations of *Bacillus subtilis* cells to low pH and a comparison of modeling approaches. *Geochim. Cosmochim. Acta* **69**, 1123–1132.

Fein J. B., Daughney C. J., Yee N. and Davis T. A. (1997) A chemical equilibrium model for metal adsorption onto bacterial surfaces. *Geochim. Cosmochim. Acta* **61**, 3319–3328.

Fowle D. A. and Fein J. B. (2000) Experimental measurements of the reversibility of metal–bacteria adsorption reactions. *Chem. Geol.* **168**, 27–36.

Francis A. J., Gillow J. B., Dodge C. J., Harris R., Beveridge T. J. and Papenguth H. W. (2004) Uranium association with halophilic and non-halophilic bacteria and archaea. *Radiochim. Acta* **92**, 481–488.

Gadd G. M. (2010) Metals, minerals and microbes: geomicrobiology and bioremediation. *Microbiology* **156**, 609–643.

Gorman-Lewis D., Martens-Habbena W. and Stahl D. (2019) Cu (II) adsorption onto ammonia-oxidizing bacteria and archaea. *Geochim. Cosmochim. Acta* **255**, 127–143.

Joe-Wong C., Shoenfelt E., Hauser E. J., Crompton N. and Myneni S. C. B. (2012) Estimation of reactive thiol concentrations in dissolved organic matter and bacterial cell membranes in aquatic systems. *Environ. Sci. Technol.* **46**, 9854–9861.

Kenney J. P. L., Song Z., Bunker B. A. and Fein J. B. (2012) An experimental study of Au removal from solution by non-metabolizing bacterial cells and their exudates. *Geochim. Cosmochim. Acta* **87**, 51–60.

Krader P. and Emerson D. (2004) Identification of archaea and some extremophilic bacteria using matrix-assisted laser desorption/ionization time-of-flight (MALDI-TOF) mass spectrometry. *Extremophiles* **8**, 259–268.

Labrenz M., Druschel G. K., Thomsen-Ebert T., Gilbert B., Welch S. A., Kemner K. M., Logan G. A., Summons R. E., De Stasio G., Bond P. L., Lai B., Kelly S. D. and Banfield J. F. (2000) Formation of sphalerite (ZnS) deposits in natural biofilms of sulfate-reducing bacteria. *Science* **290**, 1744–1747.

Ledin M., Pedersen K. and Allard B. (1997) Effects of pH and ionic strength on the adsorption of Cs, Sr, Eu, Zn, Cd, and Hg by *Pseudomonas putida*. *Water Air Soil Pollut.* **93**, 367–381.

Lipp J. S., Morono Y., Inagaki F. and Hinrichs K. U. (2008) Significant contribution of Archaea to extant biomass in marine subsurface sediments. *Nature* **454**, 991–994.

Mishra B., Boyanov M., Bunker B. A., Kelly S. D., Kemner K. M. and Fein J. B. (2010) High- and low-affinity binding sites for Cd on the bacterial cell walls of *Bacillus subtilis* and *Shewanella oneidensis*. *Geochim. Cosmochim. Acta* **74**, 4219–4233.

Naik S. and Furtado I. (2014) Equilibrium and kinetics of adsorption of $Mn^{2+}$by haloarchaeon *Halobacterium* sp. GUSF (MTCC3265). *Geomicrobiol. J.* **31**, 708–715.

Pitzer K. S. (1973) Thermodynamics of electrolytes. I. Theoretical basis and general equations. *J. Phys. Chem.* **77**, 268–277.

Rai D., Felmy A. R., Juracich S. P. and Rao L. F. (1995). In *Solubilities of actinide solids under oxic conditions. Report*, SAND 94–1949, Sandia National. Laboratory, Albuquerque, New Mexico.

Rothschild L. J. and Mancinelli R. L. (2001) Life in extreme environments. *Nature* **409**, 1092–1101.

Seders L. A. and Fein J. B. (2011) Proton binding of bacterial exudates determined through potentiometric titrations. *Chem. Geol.* **285**, 115–123.

Showalter A. R., Szymanowski J. E. S., Fein J. B. and Bunker B. A. (2016) An x-ray absorption spectroscopy study of Cd binding onto a halophilic archaeon. *J. Phys.: Conf. Ser.* **712**, 012079.

Sun Y., Zhang R., Ding C., Wang X., Cheng W., Chen C. and Wang X. (2016) Adsorption of U(VI) on sericite in the presence of *Bacillus subtilis*: A combined batch, EXAFS and modeling techniques. *Geochim. Cosmochim. Acta* **180**, 51–65.

Swanson J. S., Reed D. T., Ams D. A., Norden D. and Simmons K. A. (2012) Status report on the microbial characterization of halite and groundwater samples from the WIPP. Report LA-UR 12-22824. Los Alamos National Laboratory; Carlsbad, NM.

Voica D. M., Bartha L., Banciu H. L. and Oren A. (2016) Heavy metal resistance in halophilic bacteria and archaea. *FEMS Microbiol. Lett.* **363**. https://doi.org/10.1093/femsle/fnw146.

Walsh M. J. and Ahner B. A. (2013) Determination of stability constants of Cu(I), Cd(II) & Zn(II) complexes with thiols using fluorescent probes. *J. Inorg. Biochem.* **128**, 112–123.

Westall J. C. (1982) FITEQL, A computer program for determination of chemical equilibrium constants from experimental data. Version 2.0. Report 82–02, Dept. Chem., Oregon St. Univ., Corvallis, OR, USA.

Yee N. and Fein J. (2001) Cd adsorption onto bacterial surfaces: A universal adsorption edge? *Geochim. Cosmochim. Acta* **65**, 2037–2042.

Yu Q. and Fein J. B. (2015) The effect of metal loading on Cd adsorption onto Shewanella oneidensis bacterial cell envelopes: The role of sulfhydryl sites. *Geochim. Cosmochim. Acta* **167**, 1–10.

Yu Q. and Fein J. B. (2016) Sulfhydryl binding sites within bacterial extracellular polymeric substances. *Environ. Sci. Technol.* **50**, 5498–5505.

Yu Q. and Fein J. B. (2017) Controls on bacterial cell envelope sulfhydryl site concentrations: The effect of glucose concentration during growth. *Environ. Sci. Technol.* **51**, 7395–7402.

Yu Q., Szymanowski J., Myneni S. C. B. and Fein J. B. (2014) Characterization of sulfhydryl sites within bacterial cell envelopes using selective site-blocking and potentiometric titrations. *Chem. Geol.* **373**, 50–58.

Associate editor: Oleg S. Pokrovsky